City Research Online

City, University of London Institutional Repository

Experimental and modeling investigations of the phase behavior and densities

of diesel + nitrogen mixtures

Aaron J. Rowane[a], Ashutosh Gupta[b], Manolis Gavaises[a], Mark A. M[c]Hugh[c,*]

[a]   Department of Mechanical Engineering and Aeronautics, City University of London,

Northampton Square, ECIV 0HB London, UK

[b]   Afton Chemical Corporation, 500 Spring Street, Richmond, VA 23219

[c]   Department of Chemical and Life Science Engineering, Virginia Commonwealth University,

     601 W Main St, Richmond, VA, 23284

[*]   Corresponding Author

Abstract

It has been recently speculated that diesel injection into a supercritical air environment at high-pressure, high-temperature (HPHT) conditions results in the diesel + air mixture transitioning into a single supercritical fluid phase. To help resolve this issue we report HPHT isothermal bubble (BP) point data from ~300 to 530 K and pressures to ~160 MPa for three different types of diesel fuels in N_2 that is considered a surrogate for air. One of the diesels (Highly Paraffinic, HPF) has a larger paraffinic content relative to the others, another (Highly Aromatic, HAR) has a larger aromatic content relative to the others, and the third is a Ultra-Low Sulfur Diesel (ULSD) that resembles an unfinished commercial diesel. In addition, isothermal, density data are also reported at pressures from the BP to ~165 MPa for mixtures with N_2 content ranging from ~ 3 to 55 wt%. The *T, p* range of the experimental data are extended with model calculations using the PC-SAFT

equation of state (EoS) with pseudo-component parameters for diesel. Both types of diesel + N_2 mixture data provide a rational basis for determining values for k_{ij}, a binary mixture parameter needed for EoS calculations. Modeling results show that the temperatures predicted for diesel + N_2, supercritical fluid behavior can vary significantly depending on the method used to characterize the EoS properties of the complex diesel mixtures. Nevertheless, the predicted critical-mixture curves provide useful insight for interpreting the results from supercritical diesel spray investigations.

Key words: High Temperature, High Pressure, Diesel Phase Behavior, Density, Bubble Points

1. Introduction

The benefits of high-pressure, high-temperature (HPHT) supercritical diesel injection are the disappearance of the gas-liquid interface, enhanced mass transfer between the gas and liquid phases, and zero latent heat of vaporization[1]. Supercritical diesel injection could potentially reduce emissions, minimize pollutant formation, and ultimately increase engine efficiency[2]. There are several experimental studies that report on the feasibility of supercritical injection at combustion chamber conditions. The approach taken in a majority of these studies is to investigate the differences observed in spray structures for diesel surrogates and commercial diesels when varying experimental parameters such as the injection pressure, chamber pressure, and chamber temperature. The spray experiments typically are performed at fixed combustion chamber conditions set to match expected subcritical or supercritical conditions that are often estimated using available equations of state (EoS). For example, Wensing et al.[3] and Falgout et al.[4] both use a cubic EoS to estimate operating conditions needed to achieve a single fluid phase for select diesel

surrogates + N_2 systems. Although both Wensing et al. and Falgout et al. also study diesel + N_2 spray systems they do not estimate the conditions where a single phase may be expected due to the complexity of these mixtures which may that contain hundreds of compounds. Both studies evaluate the resultant fuel spray images to determine whether or not the fuel + N_2 mixture exhibits critical behavior. It is interesting to note that Wensing et al. assert that the two-phase, diesel + N_2 system transitions to a single supercritical fluid phase while Falgout et al. report that the two-phases do not transition to a single supercritical fluid phase. For these two studies neither group reports detailed diesel compositional information, which makes it problematic for calculating the conditions needed to obtain a supercritical fluid phase for diesel in the presence of N_2.

Improving diesel engine combustion efficiency is at the core of the forthcoming Euro VII regulations, which will demand reduction of emissions from all types of diesel powertrains. Understanding the impact of changes in pressure and temperature on fuel properties is vital for simulating various processes relevant to Diesel injection and combustion. Properties such as density, viscosity, speed of sound and bulk modulus affect the injection process and phase-changing phenomena within the fuel injector, which in turn, control soot emission levels[5]. In addition, recent studies have shown that injection against air at supercritical conditions, relative to the liquid fuel, can improve combustion and reduce emissions further[6, 7]. Currently there is limited information available for diesel fuel properties as a function of pressure and temperature at diesel engine operating conditions (see for example[8, 9]). To the best of our knowledge there are no experimental studies that report diesel + N_2 mixture density or phase behavior data at HPHT conditions. It is important to note that both the temperature and pressure of diesel engines can vary and are dependent on the speed and load of engine operation. Two studies[10, 11] (selectively, among many others) summarize the conditions that prevail during a typical injection in modern engines

where the chamber gas temperature is shown to be ~700 K prior to the flame arrival. However, Vogel et al.[7] speculate that at the greatest engine loads, when the piston reaches top dead center the combustion chamber conditions can exceed 10 MPa and 1000 K. Recent spray studies by Crua et al.[12] for n-alkane diesel surrogates show that for injection of *n*-hexadecane into an air surrogate mixture (89.71% N_2, 6.52% CO_2, and 3.77 % H_2O) at conditions exceeding ~9 MPa and ~1000 K the *n*-hexadecane + air mixture exhibit a diffusive mixing process implying that the mixture within the chamber has achieved a supercritical state.

In the present study, mixture densities and phase behavior data at HPHT are obtained for mixtures of three different diesels with N_2. One of the diesels (Highly Paraffinic, HPF) has a larger paraffinic content relative to the others, another (Highly Aromatic, HAR) has a larger aromatic content relative to the others, and the third is a Ultra-Low Sulfur Diesel (ULSD) that resembles an unfinished commercial diesel. Detailed composition information is provided for all three diesels. The mixture densities are obtained in the single-phase region and these data are correlated with a modified Tait equation. Isothermal bubble point (BP) data are also obtained and these data are correlated with an Antoine-type equation. Both correlations provide reliable and facile means of data interpolation needed for easy comparison to model predictions and to literature data that becomes available in the future. The Perturbed Chain Statistical Associating Fluid Theory (PC-SAFT) EoS[13] is used to model the resultant mixture densities and phase behavior data. Two different group contribution (GC) methods are used to calculate the PC-SAFT EoS pure component parameters assuming the multi-component diesel can be represented as a single, pseudo-component as described by Rokni et al.[14,15] . One set of calculations are performed with the GC method of Sauer and coworkers[16] (S-GC), who regressed GC parameters from a large data set of PC-SAFT parameters obtained by fitting pure component, vapor pressures and saturated

liquid densities. The S-GC parameter database is weighted toward low pressures since the critical

pressures for most of the hydrocarbons found in diesel rarely exceeds 3.0 MPa. The other set of

calculations are performed with the GC method of Burgess and coworkers[17] (B-GC), who

regressed GC parameters from pure component, HPHT densities. The B-GC parameter database

is weighted toward HPHT calculations at conditions similar to those measured in the present study.

The PC-SAFT model is also used to predict the pressure-temperature (p-T) locus of the mixture-

critical curves for the diesel + N_2 systems to show the HPHT conditions needed for these mixtures

to enter a single, supercritical fluid state. These calculations address the important issue of whether

diesel + N_2 transition to a supercritical fluid state exhibiting the previously described inherent

benefits of supercritical injection.

2. Materials and Methods

2.1. Materials

Table 1 lists the hydrogen to carbon ratio, $R_{H/C}$ and average molecular weight, M_{ave}, for the

fuels used in this study as determined from gas chromatography analysis results[18, 19] (Triton

Analytical Corporation). Table 2 provides information on the amount of n-paraffins, i-paraffins,

saturated cyclics, aromatics, naphthoaromatics, and heteroatoms found in the three diesels, with

further details given elsewhere[20].

Table 1. Hydrogen to carbon ratio, $R_{H/C}$, and average molecular weight, M_{ave}, for HPF, ULSD, and

HAR diesels investigated in this study.

Diesel	$R_{H/C}$	M_{ave}/g•mol^{-1}
HPF	1.91	212.0

ULSD	1.89	199.9	
HAR	1.81	194.5	

Table 2. Total weight percent, W_{CF}, for each chemical family in each fuel.

	W_{CF}/%		
Chemical Family	HPF	ULSD	HAR
n-Paraffins	8.00	13.11	13.01
i-Paraffins	28.36	18.06	13.53
Saturated Cyclics	45.08	50.91	46.87
Aromatics	15.85	9.93	17.38
Naphthoaromatics	2.63	7.93	9.07
Heteroatoms	0.1	0.2	1.1

2.2. Experimental Methods

The apparatus and techniques used to measure HPHT BP and density measurements for each diesel + N_2 mixture are described in detail elsewhere[21-24] and are only briefly presented here. Figure 1 shows the variable-volume, view cell that is the major component of the apparatus. A pressure generator delivers or removes water to the back end of the cell and to a pressure gauge for measurements less than ~65 MPa (Model CM57303, 0 - 68.9 MPa, standard uncertainty of 0.07 MPa, Heise Corporation), and to a transducer for measurements greater than ~65 MPa (Model 245BWGDNEAPW, 0 - 345 MPa, standard uncertainty of 0.34 MPa, Viatran Corporation). The system pressure is equal to the water pressure plus/minus 0.07 MPa needed to move the o-ring-sealed, floating piston forward/backward. The cell temperature is typically maintained to within ±

0.30 K as measured with a type-K thermocouple calibrated against a calibrated RTD thermometer (Model DURAC TP-R04, range 173 to 673 K, permissible deviation of 0.06 K, H-B Instrument Company). The diesel + N_2 mixture in the cell is mixed with a stir bar controlled by an external magnet/motor located underneath the cell. The contents of the cell are projected onto a video monitor using a camera (Model STC-N63CJ, Lenox Instrument Company) coupled to a borescope (Model HAWKEYE® Pro, Gradient Lens Corporation) placed against the sapphire window (Hemlite sapphire, GT Crystal Systems, LLC) sealed with an elastomeric o-ring at the front end of the cell.
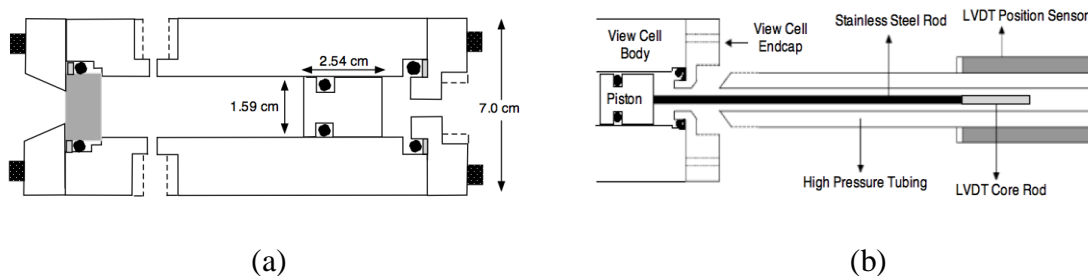

(a)   (b)

Figure 1. Schematic diagram of (a) the high-presssure variable-volume, view cell and (b) the rod connecting the piston to the LVDT (not to scale).

For BP and density measurements, the empty cell is flushed three times with N_2 at ~2 MPa to reduce the residual oxygen content to less than 10 ppm. After flushing, typically 0.025 g N_2 remains in the cell. Approximately 2.0 to 10.0 g of liquid diesel fuel are charged to the cell using a syringe weighed (± 0.001 g) before and after loading. Next, ~ 0.7 to 2.0 g of N_2 are loaded using a high-pressure, transfer vessel weighed (± 0.001 g) before and after loading. The final mass of N_2 in the cell includes any N_2 remaining in the cell at ambient pressure.

2.2.1. BP Measurements

At the desired temperature the cell contents are stirred vigorously for ~30 minutes to ensure thermal equilibrium. At a constant temperature, with a clear, single phase in the view cell, the system pressure is slowly reduced by ~0.5 MPa and the mixture again is stirred vigorously and allowed to come to thermal equilibrium. If a clear, single phase exists at this lower pressure, the system pressure is again slowly decreased by ~0.5 MPa and the mixture is again stirred vigorously and allowed to come to thermal equilibrium. This pressure reduction technique is continued until a small vapor bubble (BP) appears. The pressure is now increased well into the single-phase region and the solution is mixed to return to equilibrium. The pressure reduction technique is repeated with smaller step changes in pressure, several times, to reproduce the transition and to reduce the clear-to-two phase pressure interval. At the BP the composition of the liquid phase is considered equal to the overall solution composition since the bubble mass is negligible. Data are obtained at random pressures at a fixed, constant composition (isopleth) to minimize any potential experimental artifacts in the measurements.

2.2.2 Diesel Vapor Pressure Measurements

The neat diesel vapor pressure is measured by Alcor Labs using the isoteniscope method or D2879 – 18[25]. The isoteniscope technique provides measurements from $1.33 \bullet 10^{-4}$ to 0.1 MPa and 623 K. Note that the ASTM document for D2879 – 18 does not provide an estimated uncertainty of the measurements. Values for the vapor pressure of the neat diesel are listed in the supplemental information.

2.2.3. Density Measurements

The internal cell volume is determined using a linear variable differential transformer (LVDT, Model 2000 HR, Measurement Specialties Inc.) that tracks a magnetic core at the end of a rod connected to the piston as shown in Figure 2. The piston position is correlated to the internal cell volume by calibration with hexane performed over the entire *p-T* range of interest in this study. Densimeter volume data are obtained at each *P*, *T*, and LVDT reading by dividing the known mass of hexane added to the cell with accurate hexane density data obtained from the NIST REFPROP program[26, 27]. Single-phase, diesel + N_2 density data are calculated knowing the mass in the cell and the internal cell volume obtained from the LVDT calibration equation. Isothermal, isopleth density data are recorded in the single–phase region from the BP pressure to as high as ~165 MPa and temperatures from ~ 300 to 535 K. For each isotherm, pressures are chosen in random order to minimize any experimental artifacts in the measurements. The calculated maximum weight fraction expanded uncertainty is slightly more than 0.002 and the standard uncertainties of temperature are $u(T) = 0.30$ K and pressures are $u(p) = 0.07$ MPa for $p < 68.9$ MPa and 0.34 MPa for $68.9 < p < 165$ MPa. The expanded accumulated experimental uncertainty in the reported mixture densities is $U_c(\rho) = 0.80\%$ with a coverage factor, $k = 2$, which corresponds to a confidence interval of approximately 95%.

3. Experimental Results

The SI provides detailed data tables for BP transitions at a given *p*, *T*, and N_2 mole (x_{N2}) and weight (w_{N2}) fractions for all of the diesel + N_2 mixtures. The 76 BP temperatures are held within ± 0.3 K except for two HPF + N_2 points at 10.6 wt% N_2 (w_{N2}%), two ULSD + N_2 points at 25.4 w_{N2}% and 494.0 ± 0.7 K and 28.9 w_{N2}% and 524.2 ± 0.4 K, and two HAR + N_2 points at 25.4

w_{N2}% BP and 494.0 ± 0.7 K and 28.9 w_{N2}% BP and 524.2 ± 0.4 K. Figure 2a shows p-T isopleths, that are transitions at constant composition, for HPF + N_2 mixtures, Figure 2b shows isopleths for ULSD + N_2 mixtures, and Figure 2c shows isopleths for HAR + N_2 mixtures. Each isopleth is the locus of BP points that represent the transition from a single-phase region at pressures above the curve to a two phase, liquid + vapor phase region at pressures below the curve.
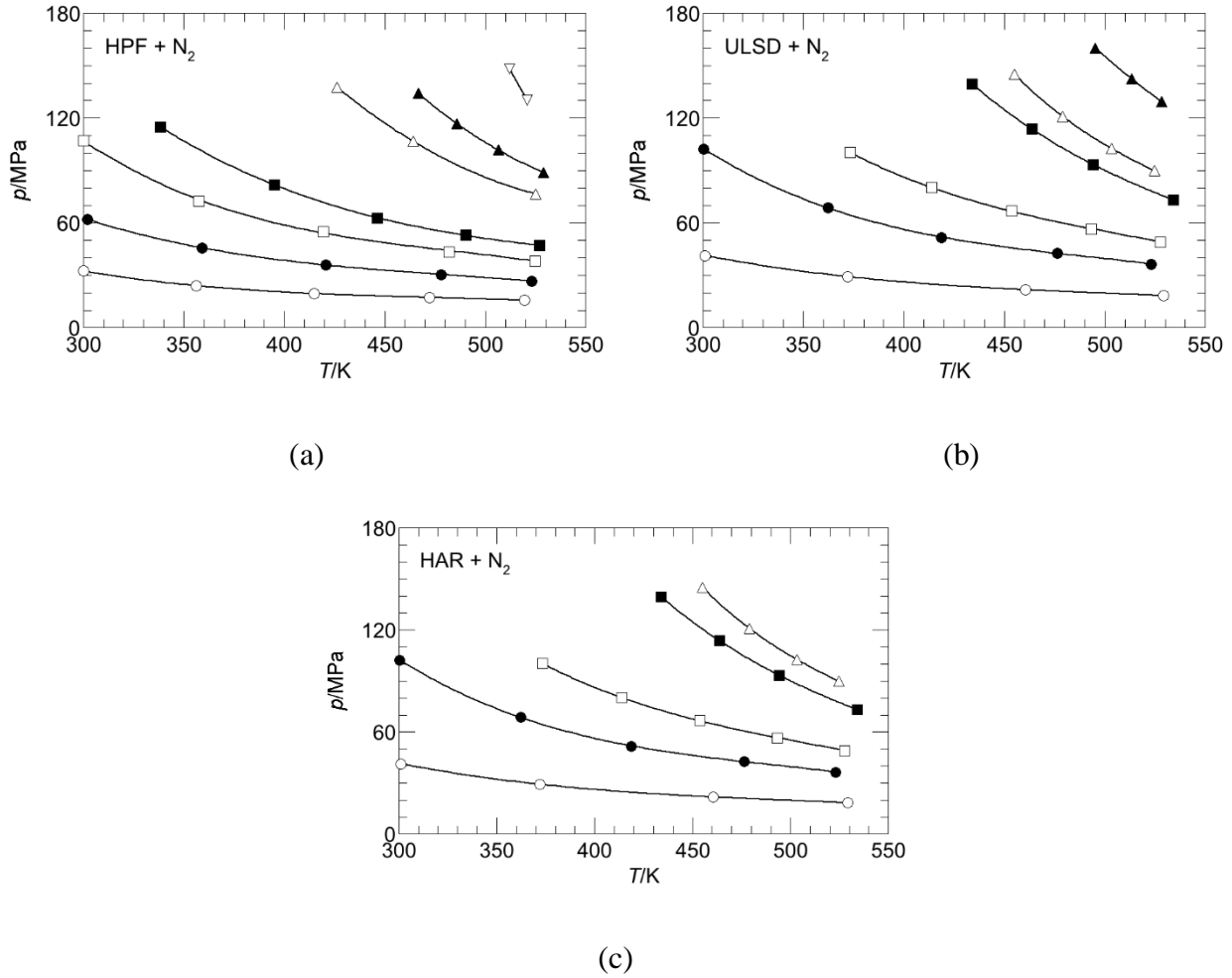

(a)

(b)

(c)

Figure 2. Pressure-temperature isopleths obtained in this study for (a) HPF + N_2 mixtures where ○ - 4.3, ● - 7.1, □ - 10.6, ■ - 13.7, △ - 23.6, ▲ - 29.2, and ▽ - 53.0 w_{N2}%, (b) ULSD + N_2 mixtures where ○ - 4.6, ● - 10.1, □ - 15.3, ■ - 25.4, △ - 28.9, ▲ - 53.6 w_{N2}%, and (c) HAR + N_2 mixtures where ○ - 2.7, ● - 12.1, □ - 20.6, ■ - 30.0, and △ - 49.3 w_{N2}%. Lines are drawn to guide the eye.

10

Figure 3a shows select p-w_{N2} isotherms for the HPF + N_2 system obtained by cross-plotting isopleth data at specific temperatures shown in Figure 2. The large positive slopes of the p-w_{N2} isotherms at temperatures below 523 K in Figure 3a clearly shown that only a modest amount of N_2 dissolves in HPF even at pressures as high as ~100 MPa. The p-w_{N2} isotherms at 373 to 473 K are also very close together reflecting the lack of temperature sensitivity for N_2 solubility at pressures to ~100 MPa. Both the large positive slopes and lack of temperature sensitivity makes it challenging to precisely measure BP data for this sparingly soluble gas in HPF at relatively low temperatures. However, note that the p-w_{N2} isotherm at 523 K is now more sensitive to pressure and begins to show characteristics of a maximum with respect to mass fraction near 125 MPa. Note that the 523 K isotherm in Figure 3a appears to approach a maximum although the maximum should not be construed to be a mixture-critical point since diesel is a multicomponent mixture and liquid-vapor tie-lines on this isotherm are not constrained to be horizontal. In addition, critical opalescence was not observed at the highest p-w_{N2} point, one of the prerequisites for a mixture-critical point[28]. Nevertheless, most of the trends observed with the p-w_{N2} isotherms for the multicomponent HPF + N_2 mixtures are nearly identical to those exhibited for the binary hexadecane + N_2 or heptamethylnonane + N_2 mixtures reported previously[29].
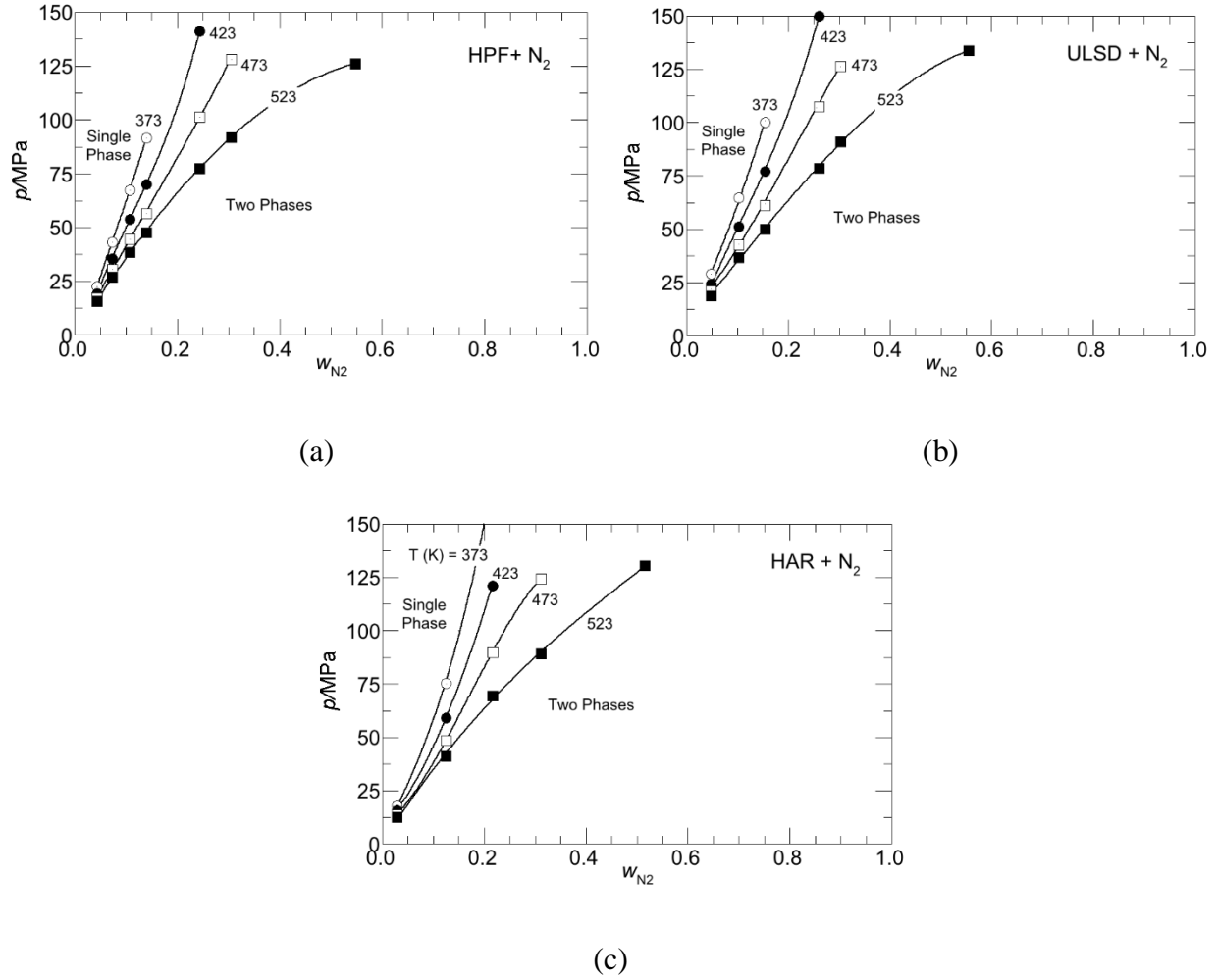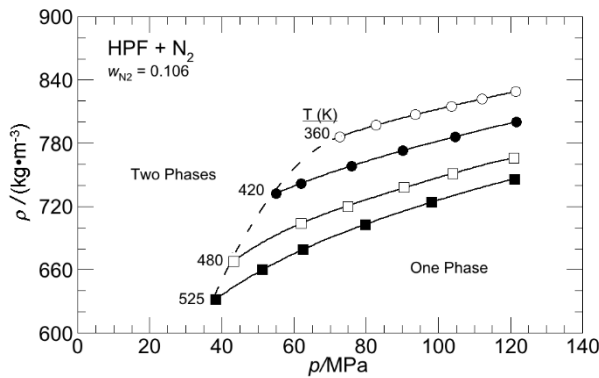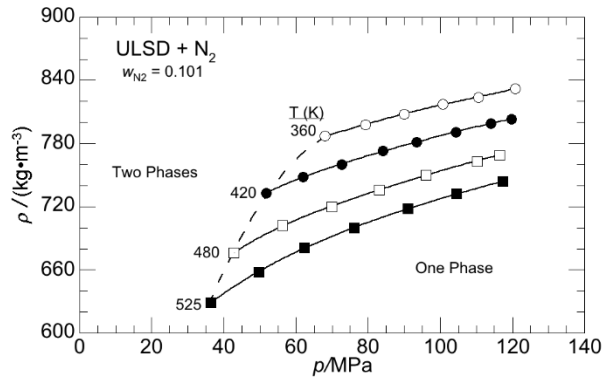
(a)   (b)

(c)

Figure 3. P-w_{N2} isotherms at 373, 423, 473, and 523 K obtained by cross plotting p-T isopleths for

(a) HPF + N_2, (b) ULSD + N_2, and (c) HAR + N_2 mixtures obtained in this study. Lines

are drawn to guide the eye.

Figure 3b and 3c show companion p-w_{N2} isotherms for ULSD + N_2 and HAR + N_2

mixtures, also at the same four temperatures shown for the HPF + N_2 system in Figure 4a. All three

diesel + N_2 mixtures exhibit very similar HPHT behavior. It is evident that less than ~ 15 w_{N2}%

dissolves in these diesel fuels when operating at pressures below 20 to 30 MPa and temperatures
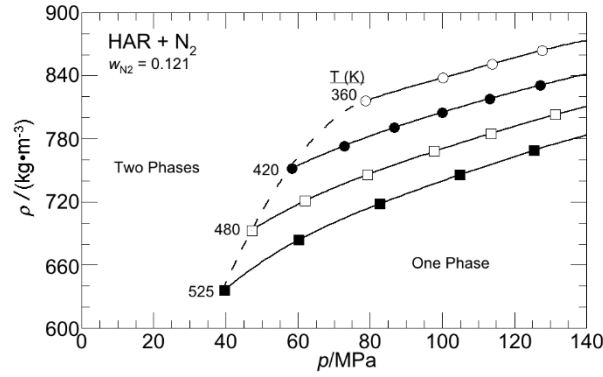
up to ~523 K.

The SI provides p-T-x_{N2}-w_{N2} data tables for mixture densities at a given p, T, x_{N2}, and w_{N2} for HPF + N_2 (164 data points), ULSD + N_2 (138 data points), and HAR + N_2 (122 data points). The mixture density data are at N_2 weight fractions from 0.027 to 0.536, pressures to ~165 MPa, and temperatures to ~535 K. Figure 4 shows an example of the effect of pressure and temperature on the density of HPF + N_2 (Figure 4a), ULSD + N_2 (Figure 4b), and HAR + N_2 mixtures (Figure 4c) each at the same temperatures, but at slightly different, fixed mixture compositions. Each density curve originates at the two-phase, BP boundary of the respective system and extends to ~120 to 140 MPa and temperatures from ~360 to 525 K. The density curves exhibit the expected trends with increasing temperature and pressure. Note that the HAR + N_2 densities are greater than those for either ULSD or HPF mixtures, even though the HAR + N_2 system has a larger amount of dissolved N_2. The higher density for the HAR + N_2 system is likely a consequence of the higher aromatic and naphthoaromatic content of HAR relative to the amounts in the other two diesels (~26 versus 17 wt%) since aromatics exhibit higher densities compared to paraffins.

(a)

(b)

(c)

Figure 4. Examples of the effect of pressure and temperature on experimental densities for each diesel + N_2 (~ 10 $wt\%$) (a) HPF, (b) ULSD, and (c) HAR where $\bigcirc$ ~ 360, $\bullet$ ~ 420, $\square$ ~480, $\blacksquare$ ~ 525 K. Lines are drawn to guide the eye.

3.1 Data Correlation

Correlation equations are used to facilitate interpolating pressure-composition (p-x) and density-composition (ρ-x) data and to generate plots of the data. Reliable correlations also provide an effective means to compare any reported phase behavior and mixture density data. In the present study BP data are correlated with an Antoine's-type equation and mixture density data are correlated with a Tait-type equation.

3.1.1 Antoine Correlation of BP Data

Equation 1 shows Antoine's equation used for interpolation of the BP data sets that allows for comparison of the results from the present study to any available literature. Values for parameters, A, B, and C, for all three diesel + N_2 systems are obtained by minimizing the percent, average, absolute deviation (Δ_{AAD}, equation 2) for p-T data at each diesel + N_2 mixture composition. The SI provides tables reporting best-fit values for these three parameters along with

14

Δ_{AAD} and maximum deviation (Δ_{max}, equation 3) values. The fit of Antoine's equation is within $\pm$ 0.6% for all 18 sets of isopleth data.

$$ln\left(\frac{p}{MPa}\right) = A - \frac{B}{T+C}$$ (1)

$$\Delta_{AAD}/\% = 100 \cdot \frac{1}{N}\sum_{i=1}^{N}\left|\frac{x_{i,exp}-x_{i,cal}}{x_{i,exp}}\right|$$ (2)

$$\Delta_{max}/\% = Max\left(100 \cdot \left(\left|\frac{x_{i,exp}-x_{i,cal}}{x_{i,exp}}\right|\right)\right)$$ (3)

where $x_{i,exp}$ is an experimental point, $x_{i,cal}$ is a calculated point, and N is the number of data points.

3.1.2 Tait Correlation of Density

Mixture density data obtained in the single-phase region are correlated using the Tait equation given by equations 4 to 6. Unlike in previous studies where the Tait reference density, $\rho_0(T)$, is calculated at $p_0 = 0.1$ MPa, here p_0 is set equal to the BP pressure at each T-x_{N2} condition calculated with Antoine's equation and best-fit parameters. Each mixture density, isothermal, isopleth is first fit to the Tait equation by varying C, $\rho_0(T)$, and $B(T)$ to minimize the Δ_{AAD} and constraining the bias (Δ_{bias}, equation 7) to zero. Once values of $\rho_0(T)$ and $B(T)$ are determined at each temperature these parameters are then fit to polynomials of temperature given by equations 4 and 5. Finally, the parameters C, a_0, a_1, a_2, b_0, b_1, and b_2 are refit simultaneously to all of the mixture density, isothermal isopleths by minimizing Δ_{AAD} and constraining Δ_{bias} to zero. The SI provides tables listing the parameters used with equations 4 to 6 for all three diesel + N_2 systems

at each mixture composition where parameters for neat diesel are from our previous study[20]. With this calculation scheme the Δ_{AAD} is less than 0.4% and the Δ_{MAX} varies from 0.3 to 1.5% at temperatures from 298 to 534 K and pressures from each respective BP to 165 MPa although the Tait equation, with appropriate parameters, is valid up to 300 MPa for the densities of the neat diesels.

$$\frac{\rho - \rho_0(T)}{\rho} = C \log_{10}\left(\frac{P + B(T)}{P_0 + B(T)}\right) \tag{4}$$

$$\rho_0(T)/kg \bullet m^{-3} = \sum_{i=0}^{2} a_i T^i \tag{5}$$

$$B(T)/MPa = \sum_{i=0}^{2} b_i T^i \tag{6}$$

$$\Delta_{bias}/\% = \frac{1}{N}\sum_{i=1}^{N} 100 \cdot \left(\frac{x_{i,exp} - x_{i,cal}}{x_{i,exp}}\right) \tag{7}$$

The Tait equation, with parameters found in the SI, is used to create Figure 5a that shows the variation of saturated, liquid-phase densities (ρ^{sat}) for HPF + N_2 mixtures as a function of N_2 content at a fixed temperature and, implicitly, as a function of pressure. Likewise, the Tait equation, with parameters reported by Rowane et al.[29], is used to create Figure 5b that shows ρ^{sat} for hexadecane (n-C16) + N_2 mixtures. The ρ^{sat} trends exhibited by HPF diesel are strikingly similar to those for pure n-C16, which is considered a diesel surrogate. In both cases the isothermal ρ^{sat} curves initially decrease as N_2 dissolves into the hydrocarbon-rich liquid phase at all temperatures from ~300 to 525 K. All of the ρ^{sat} isotherms at temperatures less than 500 K for HPF diesel and for n-C16 exhibit shallow minima at N_2 weight fraction of ~ 0.10 and then increase

fairly rapidly as more N_2 dissolves in the hydrocarbon-rich liquids. Note that n-C16 densities are ~10% lower than diesel densities, likely due to the saturated cyclic and aromatic content in HPF. The ρ^{sat} isotherms at ~525 K for the HPF and the n-C16 systems do not exhibit discernible minima as the density continually decreases with increasing N_2 content. The shapes of these high temperature ρ^{sat} isotherms suggests that each mixture is beginning to approach a dew point rather than a bubble point. Unfortunately, it is not possible to operate to higher N_2 mass fractions, temperatures much higher than ~ 525 K, and pressures in excess of ~ 150 MPa with the current experimental apparatus to obtain dew point data. Although not shown here, virtually identical trends and very similar absolute values are found for the ρ^{sat} isotherms for the ULSD + N_2 and HAR + N_2 systems over the same ~300 to 525 K temperature range.
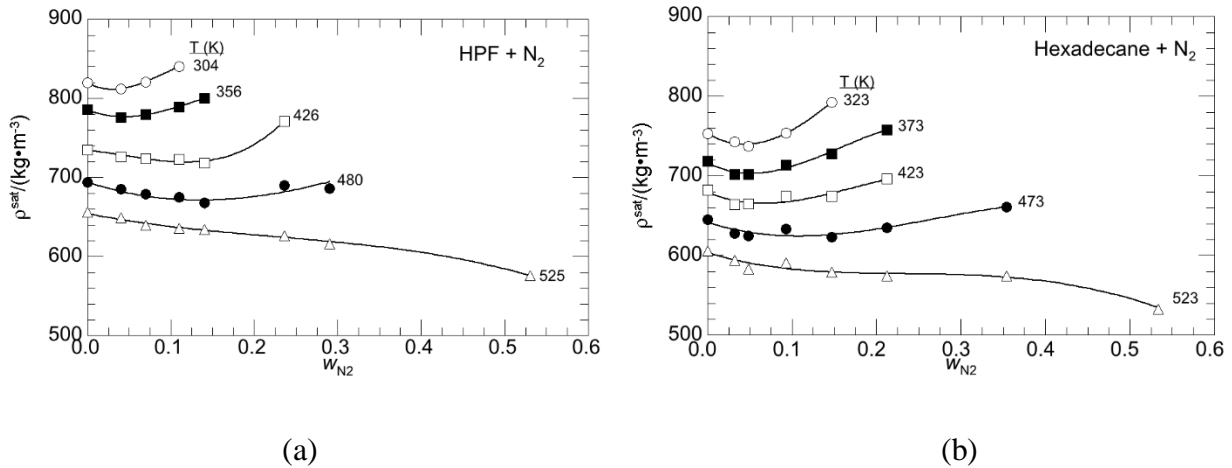

(a)   (b)

Figure 5. Variation of saturated, liquid mixture densities with N_2 content in (a) HPF + N_2 obtained in the present study; (b) Hexadecane + N_2 mixtures reported by Rowane et al.[20].

The shapes of the ρ^{sat}-w_{N2} curves reflect a balance between the reduction in liquid mixture density as N_2 dissolves into the diesel and the increase in liquid mixture density as the system pressure is increased to force N_2 into solution. This conflict of effects is exacerbated at the lowest

temperatures where N_2 is only sparingly soluble in each of the diesels as reflected in the almost vertical BP isotherms shown in Figure 3. At operating temperatures of ~ 465 K and higher, the pressure effect is a bit less pronounced since an increased amount of N_2 can more easily dissolve in the thermally-expanded diesels.

3.1.3 Modeling with PC-SAFT EoS

The PC-SAFT EoS is only briefly described here and the reader is directed to the literature for more details [13]. The EoS is derived from the residual, reduced Helmholtz free energy, a^{res},

$$a^{res} = \underbrace{a^{hs} + a^{cf}}_{a^{hc}} + a^{disp} + a^{assoc} \tag{8}$$

where a^{hs} is the hard sphere fluid contribution, a^{cf} is the chain formation contribution, a^{disp} is the dispersion interaction contributions, and a^{assoc} is the contribution from self- and cross-association complex formation, which is not applicable here since the chemical compounds found in the three diesels are not expected to self- or cross-associate with N_2. The PC-SAFT EoS requires three, pure-component parameters that are m, the number of segments in the chain, σ the temperature-independent segment diameter, and ε/k_B the interaction energy divided by Boltzmann's constant. The pure-component parameters are calculated using the methods described by Rokni et al.[14, 15], who assume that the multicomponent composition of a diesel can be characterized as a single, pseudo-component. The PC-SAFT parameters are correlated to the diesel M_{ave} and $R_{H/C}$ values shown in Table 1. Rokni uses two different group contribution (GC) methods to develop the pseudo-component correlation equations. One variation is the GC method of Burgess et al.[17] (B-

18

GC method) who use pure component HPHT density data to calculate the needed GC parameters (see Rokni et al.[14] for equation details). The other variation is the GC method of Sauer et al.[16] (S-GC method) who use pure component vapor pressure and saturated, liquid density data to calculate GC parameters (see Rokni et al.[14] for equation details). Table 3 lists both sets of PC-SAFT single, pseudo-component parameters calculated for each diesel. The results in Table 3 shows very different values for m and σ for each method, with similar values for ε/k_B. The differences in PC-SAFT parameter values reflect the different types of data and p-T regions for the data used to develop the GC parameter database. The present study assesses the performance of the PC-SAFT EoS, with the two different GC methods, to calculate diesel + N_2 mixture densities and BP data. Table 3 also lists parameters for N_2, determined from a fit of the EoS to the N_2 vapor pressure curve and saturated liquid densities, taken directly from the literature[13].

Table 3. Pseudo-component PC-SAFT parameters obtained using the Burgess (B-GC) and the Sauer (S-GC) methods.

Diesel	BGC Parameters			SGC Parameters		
	m	$\sigma/\text{Å}$	$(\varepsilon/k_B)/\text{K}$	m	$\sigma/\text{Å}$	$(\varepsilon/k_B)/\text{K}$
HPF	9.239	3.405	256.6	6.884	3.849	249.6
ULSD	8.748	3.400	256.0	6.500	3.847	250.1
HAR	8.428	3.394	260.1	6.259	3.841	253.9
N_2	1.205*	3.313*	90.96*			

*Parameters are taken directly from the literature[13].

Equations 14-16 list the combining rules[13] used to calculate a mixture value for m and cross terms, σ_{ij} and ε_{ij}, needed for diesel + N_2 mixture calculations. Here HPHT mixture density data are compared to predictive model calculations with k_{ij} set to zero for both GC methods since predicted mixture densities are less sensitive to variations in ε/k_B than m and σ. Subsequently BP data are modeled with zero and non-zero k_{ij} values using both GC methods since phase behavior calculations are very sensitive to variations in ε/k_B. Calculations are performed using commercially available software, VLXE[30].

$$m = \sum_i x_i m_i \tag{14}$$

where x_i is the mole fraction of component i.

$$\sigma_{ij} = 0.5(\sigma_i + \sigma_j) \tag{15}$$

$$\varepsilon_{ij} = (1 - k_{ij})\sqrt{\varepsilon_i \varepsilon_j} \tag{16}$$

3.1.4 Modeling Mixture Densities

Figure 6 illustrates the overall PC-SAFT EoS performance characterized by the Δ_{AAD} for density calculations for HPF + N_2, ULSD + N_2, and HAR + N_2 mixtures when using either B-GC or S-GC pseudo-component parameters and with $k_{ij} = 0$. Density predictions using B-GC parameters have overall Δ_{AAD} values that are ~200% lower than predictions using S-GC parameters. These better HPHT mixture density predictions found using B-GC parameters are not unexpected since Burgess et al. created the GC parameter database using HPHT density data sets, while Sauer et al. created their database from vapor pressure and saturated liquid density data. The

SI provides additional performance details for density predictions using both the B-GC and S-GC methods.
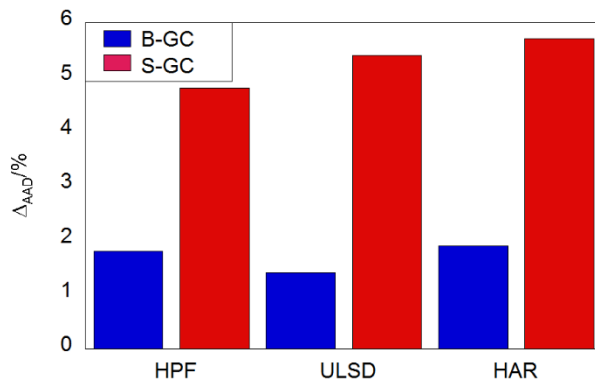

Figure 6. Overall performance of the PC-SAFT EoS when using the Burgess (B-GC) or Sauer (S-GC) pseudo-component parameters for density predictions characterized by the Δ_{AAD}.

3.1.5 Modeling VLE

Figure 7 illustrates the overall performance characterized by the Δ_{AAD} for calculated p-w_{N2} isotherms for HPF + N_2, ULSD + N_2, and HAR + N_2 mixtures using the PC-SAFT EoS with B-GC and S-GC pseudo-component parameters, both with $k_{ij} = 0$. BP predictions with Δ_{AAD} values of less than 20% are obtained with all three diesels when the B-GC pseudo-component parameters are used. In contrast, BP predictions with Δ_{AAD} values of greater than 100% for the HPF and HAR diesels and 50% for the ULSD are obtained when the S-GC pseudo-component parameters are used. If there are no data available to determine a value for k_{ij}, we recommend using the B-GC pseudo-component parameters for BP predictions of diesel + N_2 mixtures. The SI provides additional performance details for BP predictions using the B-GC or S-GC methods, both with $k_{ij} = 0$.
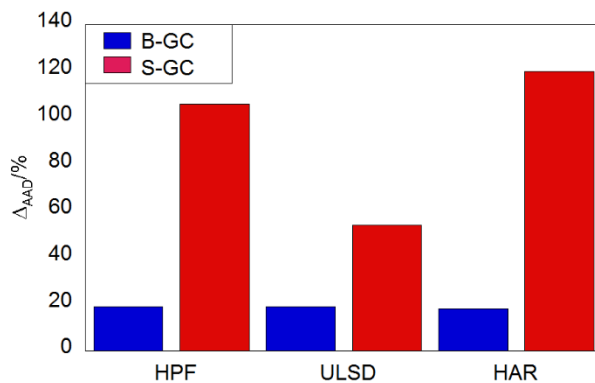
Figure 7. Comparison of Δ_{AAD} values determined from BP calculations using the PC-SAFT EoS with Burgess (B-GC) or Sauer (S-GC) pseudo-component parameters and $k_{ij} = 0$.

Table 4 lists the best-fit k_{ij} values determined from fitting p-w_{N2} isotherms with the PC-SAFT EoS and B-GC or S-GC pseudo-component parameters. Figure 8 illustrates the performance of the BP predictions, characterized by Δ_{AAD} values for HPF + N_2, ULSD + N_2, and HAR + N_2 mixtures. An improved agreement is obtained between predicted and observed phase behavior for both GC methods when a nonzero k_{ij} is used, reflecting the much higher sensitivity of phase behavior calculations to values of ε/k_B, the energetic parameter. It is interesting that the best-fit k_{ij} values for each GC method have opposite signs and different absolute values, which is a direct reflection of the impact of the very different pseudo-component parameters calculated with each GC method. The k_{ij} values found with the S-GC method are similar to those reported for PC-SAFT phase behavior calculations for hexadecane + N_2[20, 31] and heptamethylnonane + N_2 mixtures[29]. Predictions using the B-GC pseudo-component parameters have Δ_{AAD} values that are ~100% lower than those when using S-GC pseudo-component parameters. This improved performance with B-GC parameters is a result of using high pressure density data to develop the GC database rather than vapor pressure and saturated density data.

Table 4. Best-fit binary interaction parameters (k_{ij}) determined from fitting p-w_{N2} isotherms with the PC-SAFT EoS and B-GC or S-GC pseudo-component parameters.

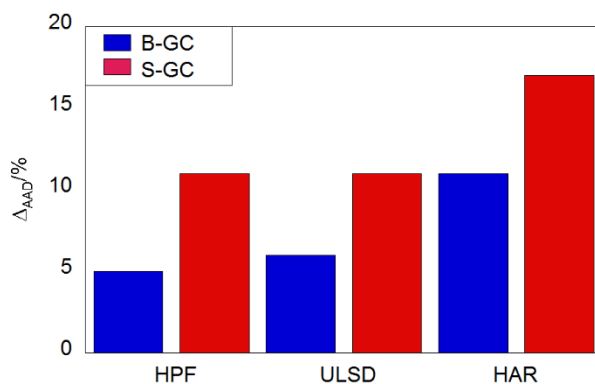|	k_{ij}	
	B-GC	S-GC
HPF	-0.0350	0.1375
ULSD	-0.0238	0.1413
HAR	-0.0313	0.1363

Figure 8. Performance of the PC-SAFT EoS when using Burgess (B-GC) or Sauer (S-GC) pseudo-component parameters for bubble-point predictions with best-fit k_{ij} values.

Although the results for both GC methods show reasonable agreement between calculated and experimental BP data, distinctly different behavior is exhibited by the calculated 473 K isotherms. A closed loop at ~170 MPa is calculated when using B-GC pseudo-component parameters, however, this same isotherm remains open even at pressures in excess of 200 MPa when using S-GC pseudo-component parameters. Note the different widths of the predicted two-phase regions of the 530 K isotherms in Figure 9. The predicted dew points (DP) using B-GC

pseudo-component parameters are richer in N_2 than similar DPs found with the S-GC parameters. At pressures less than ~10 MPa, it is reasonable to estimate the gas phase concentration using the ideal gas law since the 530 K isotherm is ~ 400 K hotter than 126.2 K, the critical temperature of N_2. Considering that the vapor pressure of HAR is expected to only be ~ 0.1 MPa at 530 K it is highly unlikely that the gas phase at this condition contains as much as 10 wt% HAR. Hence, we speculate that the 530 K isotherm predicted with B-GC parameters has a more realistic shape as compared to that predicted with the S-GC parameters.
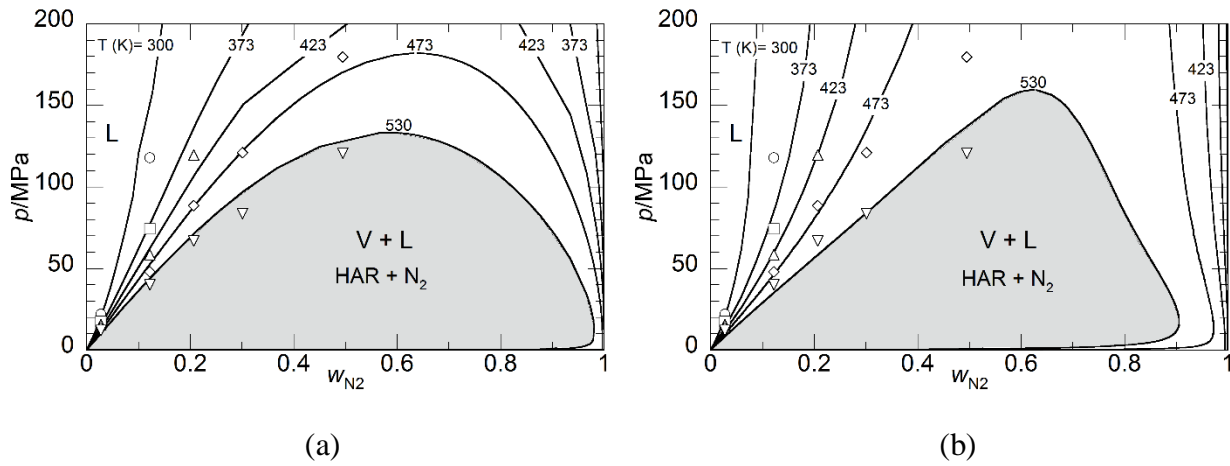

(a)   (b)

Figure 9. Comparison of experimental (symbols) and PC-SAFT calculated (lines) p-w_{N2} isotherms for HAR + N_2 mixtures with pure component parameters calculated with (a) the B-GC method and $k_{ij} = -\ 0.031$, and (b) the S-GC method and $k_{ij} = 0.136$, both at $\bigcirc$ - 300, $\square$ - 373, $\triangle$ - 423, $\Diamond$ - 473, and $\triangledown$ - 530 K. The gray area shows the two-phase, vapor + liquid region at 530 K.

Figure 10 shows p-w_{N2} isotherms predicted using the different GC methods and with k_{ij} values fit to lower temperature isotherms. The dashed line superposed on each graph intersects the maximum of the isotherms and, therefore, represents the locus of p-T-w_{N2} mixture-critical points from ~475 to 750 K for these psuedo-component + N_2 binary mixtures. As noted previously, the

24

mixture-critical point for a multicomponent, diesel + N2 mixture is not necessarily located at the maximum of the *p-x* or *p-w* isotherms so the dashed line shown here should be interpreted as estimates of the mixture-critical point. Both calculation methods show that the two-phase regions of the p-w_{N2} loops shrink as N_2 and HAR pseudo-component become more miscible as the temperature increases. However, the two-phase regions predicted with S-GC pseudo-component parameters shrink at a much faster rate with increasing temperature. These model phase behavior predictions, using a single pseudo-component to represent HAR diesel, offer reasonable estimates or bounds for the conditions needed for diesel + N_2 mixtures to transition to a single supercritical fluid phase. More accurate predictions could be obtained, at the price of more extensive computational effort, if the calculations are performed accounting for all of the many components in diesel.
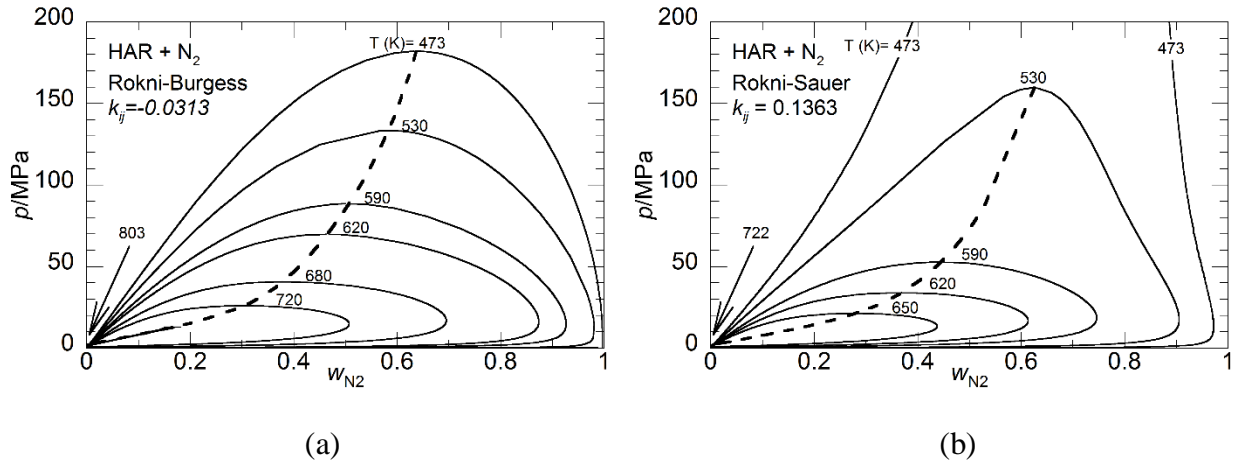

(a) (b)

Figure 10. PC-SAFT calculated p-w_{N2} isotherms for HAR + N_2 mixtures with pseudo-component parameters calculated with (a) the B-GC method and $k_{ij} = -0.0313$, and (b) the S-GC method and $k_{ij} = 0.1363$. The dashed lines through isotherm maximums represents the locus of mixture-critical points.

Figure 11 shows the *p-T* diagram for HAR + N_2 with calculated vapor pressure curves ending at the HAR critical point and with the mixture-critical curves predicted with B-GC parameters and k_{ij} = -0.031 and the S-GC parameters with k_{ij} = 0.136. The mixture-critical curve defines the *p-T* conditions needed to obtain a single phase. For this pseudo-binary mixture the mixture-critical curve exhibits a very large negative slope, indicating it is difficult to dissolve N_2 into HAR diesel even at ~ 700 K. Calculations with the B-GC parameters predict a higher HAR critical point and a two-phase region that extends to higher temperatures as compared to predictions with the S-GC parameters. Although calculations are not shown here, identical trends are obtained for the quality of the fit of the *p-w_{N2}* isotherms with k_{ij} and for the location and shape of the critical mixture curve for ULSD + N_2 and HPF + N_2 mixtures.
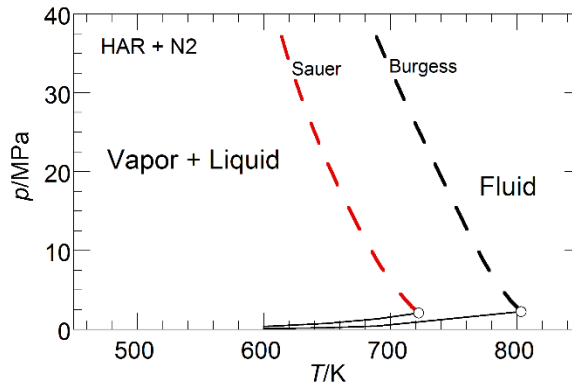

Figure 11. PC-SAFT calculated *p-T* diagram for HAR + N_2 mixtures. The HAR calculated vapor pressure curves (solid lines) ending in the critical point (circle) and the HAR + N_2 mixture critical curves (dashed lines) are calculated with the B-GC method and $k_{ij} = -0.031$ (black dashed line) and the S-GC method and $k_{ij} = 0.136$ (red dashed line).

4. Conclusions

The present study provides experimental data and modeling approaches necessary to address the important issue of whether diesel injection into a supercritical air environment ultimately results in a single supercritical fluid phase at HPHT combustion chamber conditions. These new data and modeling calculations provide needed information critical for understanding the dynamic mixing process within the diesel engine combustion chamber. The HPHT mixture density and phase behavior results for three different diesel fuels in the presence of N_2 provide a basis for modeling studies using the PC-SAFT EoS. Each diesel fuel is characterized with EoS parameters calculated using a single, pseudo-component approach incorporating two different group contribution methods. Burgess's GC method[17] provides better predictions for mixture densities and for BP data as compared to Sauer's GC[16] method since Burgess used HPHT data when developing his GC parameter database while Sauer used much lower vapor pressure and saturated liquid density data. Both types of experimental diesel + N_2 mixture data provide a rational basis for determining values for k_{ij}, a binary mixture parameter needed for the EoS calculations. Interestingly, PC-SAFT predictions using B-GC parameters provide more realistic isotherm shapes as compared to predictions using the S-GC parameters Identifying the exact T, p conditions for the mixtures to exhibit supercritical fluid behavior remains an on-going challenge given that the predicted mixture-critical curve can differ by as much ~80 K depending on the choices made to calculate the diesel EoS parameters. It is important to note that the mixture-critical pressure is very likely easily obtained in the combustion chamber since the critical pressure for most heavy hydrocarbons is typically less than 2 to 3 MPa[32] and the maximum combustion chamber pressure can exceed 15 MPa. However, the fuel + air mixture temperature prior to combustion is difficult to identify precisely since it is contingent on sufficient time for heat and mass transfer processes to occur within the combustion chamber. The temperature of the injected fuel mass is expected to

be approximately 380 K and there will be a corresponding local cooling of the surrounding air near the fuel injector. Nevertheless, critical mixture predictions for the diesel + N_2 using the GC method of Sauer et al.[16] resemble those for *n*-hexadecane + N_2 reported in our previous work[29]. Here it is assumed that the true diesel + air mixture critical curve is likely bounded between the two model variations with a uncertainty on the temperature of ± 40 K. Further, we speculate that given the diffusive mixing process observed by Crua et al.[12] at conditions exceeding 1000 K and 9 MPa for *n*-hexadecane + N_2, the diesel + air mixture could exhibit a supercritical state prior to the onset of combustion at the greatest engine load conditions when the piston reaches the top dead center in the combustion chamber[7].

References

1. Chehroudi, B.; Talley, D.; E., C., Visual characteristics and initial growth rates of round cryogenic jets at subcritical and supercritical pressures. *Phys of Fluids* **2002,** 14, 850.

2. Anitescu, G.; Tavlarides, L. L.; Geana, D., Phase transitions and thermal behavior of fuel-diluent mixtures. *Energy Fuels* **2009,** 23, 3068-3077.

3. Wensing, M.; Vogel, T.; Götz, G., Transition of diesel spray to a supercritical state under engine condtitions. *Int J Engine Res* **2016,** 17, 108-119.

4.   Falgout, Z.; Rahm, M.; Sedersky, D.; Linne, M., Gas/fuel jet interfaces under high pressures and temperatures. *Fuel* **2016,** 168, 14-21.

5.   Nikolić, B. D.; Kegl, B.; Marković, S. D.; Mitrović, M. S., Determining the speed of sound, density and bulk modulus of rapeseed oil biodiesel and diesel fuel. *Therm Sci* **2012,** 16, S569-S579.

6.   Tavlarides, L. L.; Anitescu, G. Supercritical diesel fuel composition, combustion process and fuel system. 2009.

7.   Vogel, T.; Götz, G.; Wensing, M. In *Transition of fuel components into supercritical state under diesel process condtions*, ILASS, Chania, Greece, 2013; Chania, Greece, 2013; pp 587-593.

8.   Vidal, A.; Rodriguez, C.; Koukouvinis, P.; Gavaises, M.; McHugh, M. A., Modelling of diesel fuel properties through its surrogates using PC-SAFT. *Int J Eng Res* **2018,** 257, 146808741800171.

9.   Rodriguez, C.; Rokni, H. B.; Koukouvinis, P.; Gupta, A.; Gavaises, M., Complex multicomponent real-fluid thermodynamic model for high-pressure diesel fuel injection. *Fuel* **2019,** 257, 115888.

10.   Kook, S.; Bae, C.; Miles, P. C.; Choi, D.; Pickett, L. M., The influence of charge dilution and injection timing on low-temperature diesel combustion and emissions. In SAE International: 2005.

11.   Pickett, L. M.; Genzale, C. L.; Bruneaux, G.; Malbec, L.-M.; Hermant, L.; Christiansen, C.; Schramm, J., Comparison of diesel spray combustion in different high-temperature, high-pressure facilities. **2010,** 3, 156-181.

12. Crua, C.; Manin, J.; Pickett, L. M., On the transcritical mixing of fuels at diesel engine condtions. **2017,** 208, 535-548.

13. Gross, J.; Sadowski, G., Perturbed-Chain SAFT: An equation of state based on a perturbation theory for chain molecules. *Ind Eng Chem Res* **2001,** 40, 1244-1260.

14. Rokni, H. B.; Gupta, A.; Moore, J. D.; McHugh, M. A.; Bamgbade, B. A.; Gavaises, M., Purely predictive method for density, compressibility, and expansivity for hydrocarbon mixtures and diesel and jet fuels up to high temperatures and pressures. *Fuel* **2019,** 236, 1377-1390.

15. Rokni, H. B.; Moore, J. D.; Gupta, A.; McHugh, M. A.; Gavaises, M., Entropy scaling based viscosity predictions for hydrocarbon mixtures and diesel fuels up to extreme conditions. *Fuel* **2019,** 241, 1203-1213.

16. Sauer, E.; Stavrou, M.; Gross, J., Comparison between a homo- and a heterosegmented group contribution approach based on the perturbed-chain polar statistical associating fluid theory equation of state. *Ind Eng Chem Res* **2014,** 53, 14854-14864.

17. Burgess, W. A.; Tapriyal, D.; Gamwo, I. K.; Wu, Y.; McHugh, M. A.; Enick, R. M., New group-contribution parameters for the calculation of PC-SAFT parameters for use at pressures to 276 MPa and temperatures to 533 K. *Ind Eng Chem Res* **2014,** 53, 2520-2528.

18. Dzidic, I.; Petersen, H. A.; Wadsworth, P. A.; Hart, H. V., Townsend discharge nitric oxide chemical ionization gas chromatography/mass spectrometry for hydrocarbon analysis of the middle distillates. *Anal Chem* **1992,** 64, 2227-2232.

19. Wadsworth, P. A.; Villalanti, D. C., Pinpoint hydrocarbon types new analytical method helps in processing clean fuels. *Process Technology* 1992.

20. Rowane, A. J.; Mahesh Babu, V.; Rokni, H. B.; Moore, J. D.; Gavaises, M.; Wensing, M.; Gupta, A.; McHugh, M. A., Effect of composition, temperature, and pressure on viscosities and densities of three diesel fuels. *J Chem Eng Data* **2019,** 64, 5529-5547.

21. Liu, J.; Kim, Y.; McHugh, M. A., Phase behavior of diisobutyl adipate-carbon dioxide mixtures. *Fluid Phase Equilib* **2006,** 248, 44-49.

22. Liu, K.; Wu, Y.; McHugh, M. A.; Baled, H.; Enick, R. M.; Morreale, B. D., Equation of state modeling of high-pressure, high-temperature hydrocarbon density data. *J Supercrit Fluids* **2010,** 55, 701-711.

23. Mallepally, R. R.; Gadepalli, V. S.; Bamgbade, B. A.; Cain, N.; McHugh, M. A., Phase behavior and densities of propylene + hexane binary mixtures to 585 K and 70 MPa. *J Chem Eng Data* **2016,** 61, 2818-2827.

24. Wu, Y.; Bamgbade, B. A.; Liu, K.; McHugh, M. A.; Baled, H.; Enick, R. M.; Burgess, W. A.; Tapriyal, D.; Morreale, B. D., Experimental measurements and equation of state modeling of liquid densities for long-chain n-alkanes at pressures to 265 MPa and temperatures to 523 K. *Fluid Phase Equilib* **2011,** 311, 17-24.

25. *ASTM D2879-18, Standard Test Method for Vapor Pressure-Temperature Relationship and Initial Decomposition Temperature of Liquids by Isoteniscope*. ASTM International: West Conshohocken, PA, 2018.

26. Lemmon, E. W.; Huber, M. L.; McLinden, M. O., REFPROP 9.1. **2013,** 23.

27. Lemmon, E. W.; Span, R., Short fundemental equations of state for 20 industrial fluids. *J Chem Eng Data* **2006,** 51, 785-850.

28. McHugh, M. A.; Krukonis, V. J., *Supercritical Fluid Extraction: Principles and Practice*. 2nd ed.; Butterworth-Heinemann: Stoneham, MA, 1994; p 608.

29. Rowane, A. J.; Gavaises, M.; McHugh, M. A., Vapor-liquid equilibria and densities of n-hexadecane or 2,2,4,4,6,8,8-heptamethylnonane + N2 to 535 K and 135 MPa. *Fluid Phase Equlib* **2020,** 506, 112378.

30. Laursen, T. VLXE, V. 9.3. www.vlxe.com

31. García-Sánchez, F.; Eliosa-Jiménez, G.; Silva-Oliver, G.; Vázquez-Román, R., Vapor–liquid equilibria of nitrogen–hydrocarbon systems using the PC-SAFT equation of state. *Fluid Phase Equilib* **2004,** 217, 241-253.

32. Poling, B. E.; Prausnitz, J. M.; O'Connell, J., P., *Properties of Gases and Liquids*. 5th ed.; McGraw-Hill Education: New York, 2001.